The Vertical Error Characteristics of GOES-derived Winds: Description and Impact on Numerical Weather Prediction

P. Anil Rao
University of Maryland-Baltimore County
Mesoscale Atmospheric Processes Branch
NASA/GSFC

Christopher S. Velden
Cooperative Institute for Meteorological Satellite Studies
University of Wisconsin-Madison

Scott A. Braun
Mesoscale Atmospheric Processes Branch
NASA/GSFC

Submitted to Journal of Applied Meteorology
January 2001

Corresponding author address: Dr. P. Anil Rao, University of Maryland-Baltimore County, NASA/GSFC, Code 912, Greenbelt, MD, 20771.

ABSTRACT

Errors in the height assignment of some satellite-derived winds exist because the satellites sense radiation emitted from a finite layer of the atmosphere rather than a specific level. Potential problems in data assimilation may arise because the motion of a measured layer is often represented by a single-level value. In this research, cloud and water vapor motion winds that are derived from the Geostationary Operational Environmental Satellites (GOES winds) are compared to collocated rawinsonde observations (RAOBs). An important aspect of this work is that in addition to comparisons at each assigned height, the GOES winds are compared to the *entire profile* of the collocated RAOB data to determine the vertical error characteristics of the GOES winds. The impact of these results on numerical weather prediction is then investigated.

The comparisons at individual vector height assignments indicate that the error of the GOES winds range from ~ 3 to 10 m s^{-1} and generally increase with height. However, if taken as a percentage of the total wind speed, accuracy is better at upper levels. As expected, comparisons with the *entire profile* of the collocated RAOBs indicate that clear-air water vapor winds represent deeper layers than do either infrared or water vapor cloud-tracked winds. This is because in cloud-free regions the signal from water vapor features may result from emittance over a thicker layer. To further investigate characteristics of the clear-air water vapor winds, they are stratified into two categories that are dependent on the depth of the layer represented by the vector. It is found that if the vertical gradient of moisture is smooth and uniform from near the height assignment upwards, the clear-air water vapor wind tends to represent a relatively deep layer.

The information from the comparisons is then used in numerical model simulations of two separate events to determine the forecast impacts. Four simulations are performed for each case: 1) A control simulation that assimilates no satellite wind data, 2) assimilation of all GOES winds according to their assigned single level height, 3) assimilation of all GOES winds spread over multiple levels, and 4) assimilation of all GOES winds spread over multiple levels, but with variations in the vertical influence of clear-air water vapor winds based on the moisture profile in the model. In the first case, a strong mid-latitude cyclone is present and the use of the satellite data results in improved storm tracks during the initial ~36 h forecast period. This is because the satellite data improves the analysis of the environment into which the storm progresses. Statistics for mean wind vector and height differences show that, with the exception of the height field at later times in the first case, the use of GOES winds improves the simulation with time. The simulation results suggest that it is beneficial to spread the GOES wind information over multiple levels, particularly when the moisture profile is used to define the vertical influence.

1. Introduction

The Geostationary Operational Environmental Satellites (GOES) that are currently in operation have proven to be an extraordinary source of information. GOES data have been used in a myriad of applications that includes determining vertical profiles of temperature and moisture (Ma et al. 1999), predicting convectively unstable environments (Rao and Fuelberg 1997), estimating rainfall area and volume (Anagnostou et al. 1999), estimating tropical cyclone intensity (Velden et al. 1998a), and deriving cloud properties (Turk et al. 1998). Thus, GOES data are an important tool in both weather research and forecasting.

A significant product of GOES are atmospheric motion winds that are derived by tracking either cloud or water vapor features in sequential images of satellite radiances. Although atmospheric motion winds were produced from earlier GOES series (e.g., GOES-7) (Hayden and Stewart 1987; Velden 1996), they are better suited to the lower noise, superior horizontal resolution, and greater number of channels present on the current GOES series (Nieman et al. 1997). [See Menzel and Purdom (1994) for a thorough description of the current GOES series capabilities.]

The GOES winds are produced from multispectral imagery. For example, cloud features detected in the infrared (IR) and visible (VIS) channels on the GOES imager are tracked in sequential imagery to derive wind vectors. Winds from IR typically capture flow features in both the upper- and lower-troposphere, while winds from VIS generally are used to depict motion in the lower troposphere. Water vapor (WV) features are followed using the three WV channels that are present on the current GOES satellites (i.e., 7.0 μm and 7.3 μm on the sounder and 6.7 μm on the imager). The use of three channels is appealing since motion in 3 quasi-independent layers can be estimated. These three spectral bands sense radiation emitted from slightly different layers of the mid- to upper-troposphere. While cloud features can be tracked in the WV channels as they are in IR and VIS imagery, it is also possible to track WV features in the *clear air* that occur between storm systems (Velden et al. 1997). Therefore, the full compliment of multi-spectral GOES winds provides

both dense and uniform coverage over the United States and surrounding regions. [See Velden et al. (1998b) and Nieman et al. (1997) for examples of GOES wind coverage.]

Accurate numerical weather prediction (NWP) requires observations for representing the initial state of the atmosphere and for updating the model through data assimilation. Conventional observations are relatively abundant over the continental United States (e.g., radiosondes, meso-networks, radars, etc.). This is not true over oceanic regions, where significant weather is common (e.g., cyclones off of the West Coast of the United States, hurricanes in the Atlantic basin). Thus, GOES winds are ideal for NWP since they can provide information in these important regions that would otherwise lack in accurate observations.

Many studies have shown the positive impact that GOES winds can have on NWP. For example, GOES winds were assimilated into the Geophysical Fluid Dynamics Laboratory (GFDL) hurricane prediction system to determine their impact on simulations of Atlantic hurricanes (Soden et al. 2000). In over 100 cases, the GOES winds dramatically reduced a persistent westward bias common in the GFDL model. Furthermore, the GOES winds were able to depict more accurately vorticity gyres in the environmental flow, which led to significant improvements in track position at all forecast times. These results were consistent with previous impact studies that also simulated Atlantic hurricanes. For example, assimilation of GOES winds into the Navy Operational Global Atmospheric Prediction System (NOGAPS) for four hurricanes in 1995 (Goerss et al. 1998; Velden et al. 1998b) improved forecast storm position errors by as much as 14%.

A study using the European Centre for Medium-Range Weather Forecasts (ECMWF) system showed that GOES winds are also beneficial to simulations of systems other than hurricanes (Tomassini et al. 1998). Specifically, GOES WV winds had a positive impact on the ECMWF model analyses and forecasts and led to consistent improvements in the quality of the first guess, especially in mid- and upper-levels where the winds were most prevalent. In addition, a large positive impact occurred in short-range forecasts of the tropics and Southern Hemisphere, where wind vector improvements reached 20%. In another study, the NOGAPS was used to investigate the

impact of targeted dropsondes and satellite winds on model analyses and forecasts of North Pacific weather events (Langland et al. 1999). Use of the satellite data reduced 2-day forecast errors by almost 10% during a 6-week period, thereby improving forecasts of cyclones that make landfall in the western United States. These results help illuminate the benefits of using satellite-derived winds in data sparse regions such as the North Pacific Ocean. In fact, positive impacts such as those just discussed have led to the routine assimilation of GOES winds, to varying degrees, in most operational models.

GOES winds are typically treated as single-level data, i.e., wind speed and direction at a given height. While GOES winds have had significant positive impacts on NWP, the representative height has proven to be a relatively large source of error (Nieman et al. 1993) because the satellite senses radiation emitted from a finite layer of the atmosphere rather than a specific level. Thus, potential problems in data assimilation can arise because of the difficulty in accurately representing the motion of a measured layer by a single-level value. This type of discrepancy is especially prevalent in clear-air WV winds where a sharp radiometric signal (e.g., a cloud) is not present (Velden et al. 1997; Soden et al. 2000). In addition, further complications will exist if multiple moist layers, each contributing to the radiometric signal, are present. As a result of these problems, many operational centers filter out clear-air WV winds when assimilating GOES winds into their models. In fact, only the NOGAPS currently includes these data.

The height assignment problem and the associated difficulty in properly using the GOES winds are the primary motivations for this research. While various approaches to minimizing this problem have been investigated, such as spreading the information over more than one level, the best manner in which to do this is still unknown because the vertical error characteristics of the GOES winds have not been thoroughly examined. To this end, we investigate the vertical error characteristics of these data, paying special attention to clear-air WV winds, by comparing them with collocated radiosondes and attempting to examine the depth of troposphere over which the GOES winds may be representative. This information is then used in numerical model simulations to present simple

examples of how this information can be used, and to determine its potential forecast impact. It should be noted that there are limitations to this work that will become evident in later sections, e.g., data from only one season is used to generate the statistics that are then applied to the numerical model, a historically suspect model variable (i.e., moisture) is used as a proxy in the model, and only two cases are examined. In spite of these limitations, this research is a necessary first step in understanding both the characteristics of these important data and their use in NWP. The data and methodologies used for the determination of the vertical error characteristics of the winds are described in section 2, while sections 3 and 4 describe results of the comparisons with RAOBs and numerical model simulations, respectively. Finally, section 5 presents a summary and conclusions.

2. Data and methodology

The GOES winds are produced at the Cooperative Institute for Meteorological Satellite Studies (CIMSS) at the University of Wisconsin-Madison. The datasets include information from both GOES 8 and 10 at 3-h intervals and are provided as wind speed and direction at a determined height (pressure level). Typically, IR and WV winds are produced at each time, while VIS winds are produced only at 0000 and 1800 UTC and are confined to lower tropospheric cloud tracing. The vectors are processed by automated techniques that track cloud and water vapor features in successive images of satellite radiances. Details of the tracking algorithm can be found in Nieman et al. (1997) and Velden et al. (1997, 1998b).

The height of the vector is assigned primarily by one of two techniques: the H_2O-intercept technique (Schmetz et al. 1993; Nieman et al. 1993) or comparisons between the measured radiance and a collocated model profile (Velden et al. 1997). The H_2O-intercept technique is based on the assumption that measured radiances from a single-level cloud deck from two spectral bands will vary linearly with cloud amount. Therefore, a plot of WV versus IR radiances in a region of varying cloud amount should be close to linear. The measured radiances are then compared to radiances that are calculated as a function of cloud top pressure and based on a numerical forecast of temperature

and moisture. The calculated radiances will agree with those measured by the satellite in clear and opaque cloud conditions. Thus, a cloud-top height can be inferred by comparisons between the two sets of radiances. This technique has been successful for upper-level vectors in semi-transparent cloud conditions (Nieman et al. 1993). For opaque cloud or clear-air features, the measured radiance is converted to a temperature and simply compared to a collocated model profile. The vector is assigned the height at which the satellite and model profile temperatures are equivalent.

After the initial height is determined, the height assignment can be adjusted using an automated processing system and objective quality control that analyzes the GOES wind against all other available data (e.g., model forecasts, nearby GOES winds, and aircraft observations) (Velden et al. 1997). Based on this procedure, the height assignment may be slightly adjusted to a level of "best" fit to the analyses. Typically this adjustment is less than 50 hPa.

In this study, we compare GOES winds with all available collocated radiosonde observations (RAOBs) over North America during October-December 1999. The RAOBs provide temperature, dewpoint, and wind speed and direction as functions of pressure at both mandatory and significant levels. Each RAOB was checked for data quality and required to meet the following specifications for consistency: 1) temperature, dewpoint and wind information must be reported to at least 150 hPa and 2) at least 20 data levels must be present between 850 and 200 hPa. This guaranteed data at upper levels (where the majority of GOES winds are obtained) and minimized the interpolation error for the comparisons.

The methodology consisted of first stratifying the GOES wind data by type (i.e., IR, VIS, clear-air WV, cloudy WV), and then by height assignment. Each GOES wind was then paired with the closest RAOB. To minimize discrepancies due to horizontal gradients, the pairings were required to be within one degree. It was not uncommon for a single RAOB to be within one degree of several GOES winds. If this occurred GOES winds of the same type and same height assignment were averaged and only the mean vector was used in the comparisons. For example, if three IR winds with height assignments of 300 hPa were within one degree of a single RAOB, only the mean of the

three vectors was used in the statistics. On the other hand, if two IR winds, one at 300 hPa and one at 400 hPa were present, both were used. This methodology was used since each height assignment of each GOES wind type was evaluated separately. The process resulted in approximately 200 to 700 collocated pairs of data for each height assignment of each GOES wind type. The RAOB data was interpolated to 1-hPa increments prior to the calculations.

The primary statistic used in this evaluation is the root-mean-square error (RMSE) of the mean vector difference (MVD) (Nieman et al. 1997). The MVD is defined as

$$MVD = \frac{1}{N}\sum_{i=1}^{N}(VD)_i. \tag{1}$$

Here, N is the number of observations while VD represents the vector difference, i.e.,

$$VD = \sqrt{(U_{SAT} - U_{RAOB})^2 + (V_{SAT} - V_{RAOB})^2}, \tag{2}$$

where U and V are the horizontal wind components and subscripts SAT and RAOB indicate GOES and RAOB values, respectively. The RMSE of the MVD is then written as

$$RMSE = \sqrt{MVD^2 + SD^2}, \tag{3}$$

where SD is the standard deviation about the MVD, i.e.,

$$SD = \sqrt{\frac{1}{N}\sum_{i=1}^{N}[VD_i - MVD]^2}. \tag{4}$$

After converting wind speed and direction into U and V wind components, the RMSE between the RAOBs and GOES wind for each height assignment of each wind type can then be calculated.

3. GOES winds height assignment

a. General characteristics

Figure 1 presents RMSEs for IR winds and clear-air (CA) and cloudy (CL) WV winds. Values range from ~ 3 to ~ 10 m s^{-1} and generally increase with height (Fig. 1a). This trend is at least partly due to the direct relationship between RMSE and wind speed (i.e., as wind speed

increases so should RMSE). If the RMSEs are normalized by the mean RAOB wind speed the errors tend to decrease with height with the exception of the extreme uppermost levels (Fig. 1b). Thus, if taken as a percentage of the total wind speed, the accuracy of IR and WV winds generally increases with height. These statistics for GOES winds agree with previous studies in both magnitude and trend (Velden et al. 1997; Nieman et al. 1997).

The results illustrated in Fig. 1 provide useful information about the absolute accuracy of GOES winds at their respective height assignment. However, the statistics do not explicitly convey information on the accuracy or representativeness of the height assignment. Generally, GOES winds represent flow over discrete layers (rather than single levels) of the atmosphere. The depths of these layers can vary considerably and depend on many factors. To investigate this issue, the statistics were expanded to include comparisons of the GOES winds against *all levels* of the RAOBs rather than just the height assignment (i.e., Fig. 1). These "RMSE profiles" display the accuracy of GOES winds at the height assignment with respect to all of the measured winds in a collocated vertical column of the atmosphere.

Figure 2 presents RMSE profiles of both CA and CL WV winds as well as IR winds for the 300 hPa height assignment (300 hPa results are similar to those of other height assignments). RMSE rather than normalized RMSE is shown so the actual magnitude of error could be described (profiles of each had similar shapes). If the height assignments were perfect, minimum RMSEs would occur at 300 hPa. This is not the case since slight biases (~ 30 hPa for IR and CL WV, ~15 hPa for CA WV) are present in all three profiles (Fig. 2). As expected, the RMSEs increase with distance both above and below the height assignment. However, in the upper region, the RMSEs tend to level off or decrease with height approximately 75 hPa above the height assignment. It also is evident that the profiles are relatively flat near the level of minimum RMSE. In other words, the increase of error both above and below the minimum value is gradual rather than abrupt. This result confirms that the winds represent a layer rather than just a single level of the atmosphere. This characteristic is most prevalent in the CA WV profile, which contains RMSEs that are within 2.5 m s^{-1} of the minimum

RMSE (~ 7 m s^{-1} at 315 hPa) over a ~180 hPa layer. Using the same criteria, the layers are only ~130 and ~120 hPa within the CL WV and IR profiles, respectively. Therefore, the CA WV winds have relatively smaller errors over a deeper layer than do the cloud-tracked winds. This characteristic is consistent with the profiles at upper levels where CA WV wind errors are smallest. The differences between profiles of the cloud-tracked (IR and CL WV) and CA WV winds are not unexpected since in cloud-free regions where no sharp radiometric signal is present (e.g., a cloud edge), the signal from water vapor features results from emittance over a thicker layer.

b. "Broad" and "Sharp" CA WV winds

The error profiles indicate that GOES winds are representative of more than just a single level of the atmosphere (Fig. 2) with the CA WV winds, based on Fig. 2 and radiative transfer principals, representing the deepest of these layers. Since the goal of this research is to use this information in NWP, we could simply assimilate each GOES wind on multiple model levels (rather than a single level) while weighting each level proportional to profiles like those in Fig. 2. Using this methodology, IR and CL WV winds would be assimilated over thinner layers while CA WV winds would be assimilated over relatively deeper layers. However, since the statistics are means calculated from a large number of collocated GOES/RAOB pairs, any given pair may contain a significantly different error profile than shown in Fig. 2. Therefore, errors can be introduced into the simulations if the assimilated winds are incorrectly assumed to represent a certain portion of the atmosphere.

The type of discrepancy described above could occur, for example, if a GOES wind that represents a deep region is erroneously assimilated by spreading the information only over a thin layer. Conversely, a GOES wind that truly represents a thin layer could be erroneously distributed over a much deeper region. The latter example will occur most often with CA WV winds since, in our statistical analysis, they should be assimilated over the deepest layer (Fig. 2). This example would also have the largest potential for negative impact since incorrect data are introduced into

several model levels. With that in mind, and as a means of reducing this possibility, the CA WV winds were separated into two categories. Inclusion in each category was based on the slope of the vector difference profile in a 200-hPa layer surrounding the height assignment. Specifically, slopes greater than (less than) the mean slopes of all the profiles were categorized as "broad" ("sharp"). The "broad" ("sharp") category represents profiles where RMSE values are relatively small over a deep (shallow) layer. A layer of 200 hPa was chosen since it represents the typical depth over which the CA WV wind RMSE profiles were symmetric about the height assignment (e.g., Fig 2). The RMSE profiles were then calculated for both categories, along with associated mean profiles of dewpoint depression and dewpoint depression gradient. Although this type of stratification could be done in many ways, this method allows a simple interpretation of possible deviations from the mean RMSE profiles of the CA WV winds. In addition, the relationship between the RMSE profiles and the vertical moisture distribution can be investigated.

Broad and sharp RMSE profiles were calculated for each height assignment of the CA WV winds. In general, the vertical moisture characteristics of all height assignments were similar within each category. Therefore, for brevity, only two height assignments that contained the largest differences are presented here (i.e., 300 and 400 hPa). Figure 3 shows mean broad (3a) and sharp (3b) profiles of the 300-hPa height assignments. Also shown are comparisons between representative individual members of the broad and sharp categories (Figs. 3c-e). It is clear that there are distinct differences present in the vertical moisture distribution between the broad and sharp categories (Figs. 3a-b). This is evident near and below the height assignment where the mean dewpoint depression (DD) between 300 and 500 hPa is ~11 K within the sharp category (Fig. 3b), while reaching ~20 K in the broad category (Fig. 3a). The shapes of the DD profiles are different between the two categories with the DD of the sharp category containing a minimum near the height assignment and the DD of the broad category decreasing smoothly with height. The latter difference is best illustrated in profiles of the dewpoint depression gradient (DDG), which for the broad category is negative from below the height assignment to at least 150 hPa, and for the sharp category

changes sign near the height assignment. The former reflects the smooth DD profile that contains no distinct peaks (Fig. 3a) while the latter reflects the peak in humidity at that level (Fig. 3b). The representative individual observations (Figs. 3c-e) highlight the complexities possible at any given location.

Figure 4 is similar to Fig. 3 but for the 400 hPa height assignments. Also shown are examples of individual observations, including a typical "multi-peaked" RMSE profile (Figs. 4c-e). The broad category of the 400-hPa height assignments (Fig. 4a) has similar mean characteristics to the broad category of the 300-hPa height assignments (Fig. 3a). For example, the mean DD is smooth and decreases with height from just below the height assignment. This is evident by noting the negative DDG from near the height assignment to at least 150 hPa (Fig. 4a). Another similarity is that the atmosphere is less humid near and below the height assignment than the corresponding region in the sharp category (Fig. 4b). Specifically, the mean DD between 400 and 600 hPa is ~27 K in the broad category (Fig. 4a), while only ~20 K in the sharp category (Fig. 4b).

Comparisons between the sharp categories of the 400 (Fig. 4b) and 300 hPa height assignments (Fig. 3b) indicate that the shape of the DD profiles are different, i.e., the profiles are inverted with respect to one another. However, a similarity is present between both profiles that clearly differentiate the sharp and broad categories. Specifically, similar to the 300-hPa height assignments (Fig. 3b), the DDG within the sharp category changes sign at the height assignment (Fig. 4b). While this is due to a moist layer for the 300 hPa height assignments (Fig. 3b), for 400 hPa it is a result of increasing moisture above and beneath a dry layer near 400 hPa (Fig. 4b) that results in a DDG profile that changes sign near the height assignment. Neither DDG profile within the broad category of either height assignment exhibits this characteristic (Figs. 3a and 4a). These differences between the vertical moisture structure of the broad and sharp categories are also present for other height assignments (not shown). Therefore, it is suggested that CA WV winds represent a relatively deeper layer (i.e., broad profile) when the vertical moisture gradient is smooth and of uniform sign from near the height assignment to upper levels.

Explanations for the CA WV characteristics are difficult to precisely determine due to the complex nature of remotely sensed water vapor measurements. Specifically, the amount of radiation that reaches a satellite detector in the WV spectrum and its origin is dependent on numerous factors which can include: the depth of the moisture, the height of the moist layer, the amount of moisture present, the number of moist layers in the path of the radiation, and the air temperature in the path of radiation. However, in general terms, the WV channels on GOES measure WV in the mid- to upper-levels of the troposphere. The more humid and warmer the air, the more it contributes to the total radiation received by the satellite sensor.

While keeping the generalities mentioned above in mind, more specific scenarios that relate to the broad and sharp profiles can be described. For example, if a single moist layer is present in the mid-levels, the majority of radiation that reaches the satellite will typically originate from the top of the moist layer (Weldon and Holmes 1991). Although over-simplified (this can be dependent on several factors that include the amount of moisture present and the channel that is used, e.g., the 7.3 μm channel will sense "deeper" into the atmosphere than will the 6.7 μm channel), it is this scenario that may describe the sharp category of the 400 hPa height assignments (Fig. 4b). Specifically, the radiation that reaches the satellite may originate from the increasing moisture just below the dry layer near 400 hPa. On the other hand, if the single moist layer is present in the upper-levels, the radiation typically originates from below the top of the moist layer (Weldon and Holmes 1991). While this also is over-simplified, it may describe the sharp category of the 300-hPa height assignments (Fig. 3b) since the moist layer is centered on the level of minimum RMSE (i.e., 300 hPa). In contrast to the sharp categories, the broad categories are relatively dry and free of discrete moist layers near the height assignment (Figs. 3a and 4a), so no distinct region of moisture is present and the radiation will originate from a relatively deep layer of the atmosphere.

c. Comparisons with the "natural correlation" of the wind

The broad and sharp profiles suggest that the depth of the layer represented by CA WV winds is related to the vertical moisture structure. However, it is not clear if the profiles are also dependent on the "natural correlation" of the actual wind. The term "natural correlation" (NC) describes the relationship between the actual wind at a given level and the actual winds both above and below this level. The NC profiles are calculated in the same manner as the GOES wind error profiles, but substituting the RAOB wind in place of a GOES wind at a given height assignment. If the CA WV winds and the RAOB winds at a given height assignment are identical, the resulting CA WV wind RMSE profile would be identical in shape and magnitude to the corresponding NC profile. On the other hand, if a NC profile and a corresponding CA WV wind profile are not identical, but exhibit a similar shape, it suggests that the depth of the layer represented by the CA WV wind is at least partly due to the natural correlation of the wind.

Fig. 5 presents NC profiles for the broad and sharp categories of the 300-hPa height assignments. Also shown are the corresponding CA WV profiles (i.e., Figs. 3a-b). [Note that the NC profiles are not exactly zero at 300 hPa due to slight vertical smoothing.] In general, the CA WV profiles exhibit larger RMSEs than their NC counterparts in both the broad and sharp categories (Fig. 5a-b), while the shapes of the two profiles are different in the broad category (Fig. 5a) but similar in the sharp category (Fig. 5b). In both categories, the RAOB winds at 300 hPa show little correlation with RAOB winds elsewhere in the column while in the broad category, the CA WV winds at 300 hPa exhibit some correlation with RAOB winds in a layer surrounding the height assignment. Therefore, in the broad category, the CA WV winds are more representative of some weighted average of the "real" winds in this deep layer, with the greatest weight near the center of the layer (i.e., height assignment). In the sharp category, both profiles are very similar (Fig. 5d) suggesting that the winds are more representative of a single level or thin layer. Results from section 3b suggest that the departures of the CA WV profiles from the NC profiles are related to the vertical moisture structure in the troposphere.

The results presented in this section clearly indicate that GOES WV winds better represent layers rather than single levels of the troposphere. The CA WV winds represent a deeper layer than the cloud tracked winds and vertical moisture structure can be used to determine if a CA WV wind likely represents a thin or thick layer. In order to determine the impact that these findings have on NWP, several numerical model simulations are performed and are described in the next section.

4. Numerical simulations

a. Model description and configuration

The model utilized in this study is the Penn State-NCAR mesoscale model version 5 (i.e., MM5). A complete description of the model can be found in Dudhia (1993) and Grell et al. (1995), so only a brief summary is given here. The MM5 is a nonhydrostatic, three-dimensional, primitive equation model that can be used for multi-scale prediction by using multiple levels of nesting. The vertical coordinate is terrain following and consists of dimensionless σ levels while the horizontal grid uses an Arakawa-Lamb B-staggering of the velocity terms with respect to the scalar quantities. The MM5 can be initialized with one of many large-scale analyses including the National Center for Environmental Prediction (NCEP) and ECMWF operational models. In addition, it is possible to assimilate auxiliary data such as surface observations, upper-air soundings, and any special asynoptic data during the simulation. The model contains many options for cloud microphysics, boundary layer physics, radiation, and convective parameterization.

The simulations presented here consist of one mesh of 170 x 140 grid points with 36-km horizontal grid spacing. The grid contains 27 vertical levels that stretch from the surface to 100 hPa. Since the horizontal grid spacing is too coarse to explicitly resolve convective processes, the Kain-Fritsch convective parameterization (Kain and Fritsch 1992) is utilized. This scheme is designed for scales of a few tens of kilometers and has proven successful in many modeling studies (e.g., Stensrud et al. 1995; Farfan and Zehnder 1996). The terrestrial and solar radiation are included by calculating the longwave and shortwave components of radiation at individual model levels while including the

effect of absorption and scattering due to clouds (Dudia 1989). The boundary layer physics are based on the scheme developed by Troen and Mahrt (1986) and further described by Hong and Pan (1996). Finally, the initial and lateral boundary conditions are defined by the twice-daily ECMWF global surface and upper-air analyses with 2.5-degree horizontal resolution and 21 vertical levels.

The objective of the simulations is to investigate different strategies of assimilating GOES winds based on the statistics that were discussed in section 3. In particular, we wish to determine the impacts that different vertical weighting schemes used to assimilate GOES winds have on the numerical simulations. To accomplish this, we chose Newtonian relaxation, or nudging (Stauffer and Seaman 1994; Stauffer and Seaman 1990), to assimilate the GOES winds into the model simulations. This method relaxes the model variables towards the observations based on differences between the two fields. Two approaches to this scheme typically are used: "analysis nudging", in which the model state is nudged toward analyses of the observations, and "observation nudging", in which the model state is nudged directly toward the individual observations. Since observation nudging is better suited for assimilation of high-frequency asynoptic data (e.g., GOES winds) (Stauffer and Seaman 1994), it is used here. Observation nudging is designed such that observations only influence the model variables within a predetermined temporal window and three-dimensional radius of influence. The weight that the observation has on each grid point is based on the spatial distance between the observation and grid point as well as the temporal difference between the observation time and current model time step. [Further details of the nudging technique can be found in Stauffer and Seaman (1994).]

The simulations described here utilize full weight between the observation time and ± 45 min. Between this period and ± 90 min the weighting is linearly decreased to zero. Therefore, an individual GOES wind influences the model over a 3-h period. The horizontal radius of influence is 240 km and the weighting within that radius is dependent on distance. The vertical layer of influence and corresponding weights vary within each simulation and are described in the following section.

b. Case studies- description and experiments

Two cases in the eastern Pacific Ocean, both from January 2000, are described here. The two cases were chosen since the weather events in each are quite different. The first case includes a strong extratropical cyclone while the second includes only a weak frontal system. Therefore, the impact of the GOES winds on numerical model simulations of two different weather regimes affecting the western United States can be investigated.

The first case consists of a series of mid-latitude cyclones that developed in the eastern Pacific Ocean during late January 2000. The cyclones initially traveled eastward before curving towards the north and northwest and then making landfall on the southern Alaskan coastline. The model grid contains most of the eastern Pacific Ocean, as well as Alaska, southwestern Canada, and the western United States (Fig. 6). Figure 7 presents ECMWF analyses of mean sea-level pressure (MSLP) in this region during the lifetimes of these storms. At 1200 UTC 28 January (Fig. 7a), a cyclone with minimum MSLP less than 988 hPa is present in the northeastern Pacific Ocean (denoted A). This storm developed ~ 24 h earlier (not shown) and is currently moving northeastward into the Gulf of Alaska. A slight kink in the isobars is evident to the south and west of cyclone A (denoted B). Although fairly benign at this time, this trough intensifies into a strong cyclone by 0000 UTC 29 January (Fig. 7b), by which time its minimum MSLP has decreased from over 1008 hPa (Fig. 7a) to less than 980 hPa (Fig. 7b). Cyclone A has intensified further as it advances toward the coastline but begins to decay shortly thereafter. A concurrent WV image taken from GOES-10 clearly shows both storms, with the more rapidly developing storm B having a well-defined dry slot entering from the west, indicative of the role of a strong upper-level front (Fig. 8). By 0000 UTC 31 January (Fig. 7c), cyclone B is approaching the Alaskan coastline, while another storm (denoted C) has developed in its wake. The period of simulation is taken as 1200 UTC 28 January to 0000 UTC 31 January and contains the initiation and development of cyclone B.

The second case also occurs in the eastern Pacific Ocean during January 2000. Therefore, the same model grid and configuration as that used in case 1 (Fig. 6) is used here. However, the meteorological conditions during this period (i.e., 1200 UTC 16 January – 0000 UTC 19 January) were not as intense as that during case 1. Figure 9 presents ECMWF analyses of MSLP at three time periods during case 2. At 1200 UTC 16 January (Fig. 9a), a relatively intense low-pressure center is present just off the northwestern coastline of the United States. However, by 0000 UTC 18 January (Fig. 9b), the intense low has moved out of the region and a much weaker system, with associated fronts (dotted lines), now dominates the eastern Pacific Ocean. By 0000 UTC 19 January (Fig. 9c), the low center is still in the same region as 24 h earlier (Fig. 9b), while the fronts have occluded and are slowly approaching the western United States.

These two cases are appealing for many reasons: 1) Forecasting events in the eastern Pacific Ocean is difficult because of the lack of conventional observations, but is important because of the potential impact on the western United States; 2) GOES-10 provides complete and consistent coverage over this region; 3) the benefit of GOES winds in this region is potentially large because of the aforementioned lack of conventional observations; and 4) the impact of GOES winds on the simulation of two unique events (i.e., an intense mid-latitude cyclone and a more generic frontal system) can be investigated.

Several experiments are performed for each case to investigate the impact of the GOES winds on MM5 simulations (Table 1). In the first case, emphasis is placed on cyclone B that deepened rapidly between 1200 UTC 28 January and 0000 UTC 29 January (Fig. 7). The simulations are initialized with the ECMWF 2.5° analysis at 1200 UTC 28 January (Fig. 7a) and the GOES winds are assimilated via observation nudging for 12 h at 3-h intervals, resulting in an initial forecast time of 0000 UTC 29 January (Fig. 7b). The model is then run in forecast mode for 48 h. Simulation of the second case is conducted identical to the first, but the model is initialized on 1200 UTC 16 January (Fig. 9a).

Four simulations are performed for each case. These include a control (CNTL), single-level (SNGL), multi-level (MULT), and selective (SLCT) simulations (Table 1). The CNTL simulation includes no data assimilation. The SNGL, MULT, and SLCT simulations are identical to one another with the exception of the vertical layer of influence and corresponding weights that are applied during the assimilation of the GOES winds. Specifically, SNGL assimilates all of the GOES winds at their height assignment level only, with no influence on the model levels above or below the height assignment. The MULT simulation is identical to SNGL but distributes the GOES winds over a 150-hPa layer (75 hPa above and below). The weights that are applied within the layer are proportional to RMSE profiles like those in Fig. 2, so full weight is applied at the height assignment level (minimum RMSE) and gradually decreased both above and below that level. The depth over which to apply the GOES winds can be chosen based on numerous factors. A depth of 150 hPa was chosen based upon inspection of RMSE profiles for all height assignments and all wind types that indicated that the errors typically either began decreasing with height or leveled off approximately 75 hPa above the height assignment (e.g., Fig. 2). Since it made little physical sense to give GOES data increasing influence at distances further from the height assignment, 75 hPa above the height assignment was chosen as the upper boundary. For simplicity and so equal weights could be applied both above and below the height assignment, 75 hPa below the height assignment was chosen as the lower boundary. The final experiment, SLCT, combines the technique used in MULT with the broad CA WV profiles discussed (in section 3b). Specifically, all of the cloud-tracked winds are assimilated as in MULT. If a CA WV wind is present, the collocated vertical moisture profile in the model is compared to that of the broad profile (Figs. 3a and 4a). If the moisture characteristics are similar to those of the broad profiles, the CA WV wind is distributed over a 250 hPa layer (this depth and corresponding weights are chosen in a similar fashion as described for MULT). If that is not the case, the CA WV wind is distributed as in MULT. This methodology is relatively conservative in that the winds are vertically distributed over the thickest layer only in those situations that have no indication of a peak in the vertical moisture profile.

Since conventional observations are relatively scarce in our domain, verification is accomplished by comparing the model simulations with special MM5 analyses. The analyses use the previously mentioned ECMWF data as a large-scale background while assimilating all available radiosondes, surface reports, ship reports, and buoys. The grid configuration of the verification analyses is identical to that of the numerical simulations. In addition to the observations, high-resolution GOES winds are used over both the ocean and land to improve the analyses. The inclusion of GOES winds has previously been shown to improve model analyses, especially over the ocean where conventional observations are limited (e.g., Langland et al. 1999). Therefore, we believe that this methodology provides us with realistic verification analyses for our results.

c. Case studies- results

Figure 10 presents the observed track of cyclone B in case 1 along with tracks from the four MM5 simulations. The symbols represent storm positions at 12-h intervals beginning on 0000 UTC 29 January (0 h) and ending on 0000 UTC 31 January (48 h). Between 0 and 24 h, cyclone B is observed to move steadily northeastward over the eastern Pacific Ocean. At 24 h, the storm begins a more northerly turn before rapidly accelerating northwestward into the Gulf of Alaska. All of the simulations capture the general track of the storm, but keep it too far south and east of the actual position.

The simulations using GOES winds generally contain superior storm tracks during the early forecast than does CNTL (Fig. 10). For example, SNGL contains an initial storm location that is further north and east than that in CNTL. This is followed by the storm travelling in a more northward direction during the first 12 h of the simulation. However, between 12 and 24 h, an eastward component is present in the storm path that results in a 24-h location coincident with CNTL. After this period, use of the data on only one level has a negative impact on the track simulations, noted by the inferior track of SNGL. Simulations MULT and SLCT contain similar paths to SNGL during the first 12 h of the simulation, but are better between ~12 and ~36 h. In fact,

selectively distributing the CA WV winds (SLCT) results in the best track during this interval. After ~ 36, the northwestward turn into the Gulf of Alaska is not forecast when using the GOES winds and results in final positions that are too far east.

The varying storm tracks found in the four simulations (Fig. 10) can result from many complex interactions since the data are assimilated over a 12-h integration of the model. Therefore, it is difficult to precisely determine why SNGL, MULT, and SLCT are superior to CNTL during the early forecast period, why MULT and SLCT were superior to SNGL, or why SLCT was the best of those that used GOES data. However, one possible explanation for the improvement is that in regions east and northeast of the storm, the mid-level wind flow is, in general, more southerly (and closer to observed) in the simulations that assimilated GOES winds than in CNTL. This would typically result in a more northward component in the storm track and result in a more accurate simulation.

The modification of the mid-level flow is the result of assimilation of west-southwesterly and southwesterly GOES winds at mid (~ 400 – 700 hPa) and lower levels (~900 – 700 hPa), respectively (not shown), in a region where the model winds are initially westerly. The assimilation affects SNGL, MULT, and SLCT in a similar manner and results in a more northward storm track. However, both MULT and SLCT will have more southerly wind components at mid-levels compared to SNGL since the low-level GOES winds are distributed within layers that extend to mid levels. Simulation SLCT is slightly better than MULT perhaps because of the more realistic representation of the CA WV winds. Clearly, the use of the GOES winds results in positive impacts on the 0 to ~36 h tracks of the cyclone.

Figure 11 presents the minimum sea-level pressure of the storm for the various simulations. All of the simulations are significantly weaker than the observed values throughout the forecast period and only little difference is present between the simulations. At the initial time, the simulations that use GOES wind data contain slightly degraded intensities (~ 2 – 5 hPa) compared to the control simulation. Recall that cyclone B begins its rapid development during the assimilation

period between 1200 UTC 28 January and 0000 UTC 29 January (Fig. 7a,b). The mass field in the simulations may have difficulty adjusting to the frequent addition of changing GOES winds so initial errors in surface pressure may result. Nevertheless, it is clear that the intensities of the cases with GOES wind data "catch up" to CNTL after only ~ 8 h and, in general, SLCT is the closest to reality.

These results indicate the impact that varying the vertical influence of assimilated GOES winds can have on the track and intensity of a mid latitude cyclone. Specifically, GOES data generally improve the storm track during the initial ~ 36 h forecast and use of the data over multiple levels is generally better than using the data on only a single level. In addition, selectively distributing the CA WV winds based on the vertical moisture distribution results in the most accurate storm track and intensity of those simulations that use the GOES data. While informative, the storm track/intensity results may not be the best measure of the accuracy of the simulations in a more general sense. Therefore, statistics were generated by comparing the MM5 simulations to the MM5 verification analyses. The verification region is limited to only those grid points over land since inclusion of observations (e.g., RAOBs, surface reports) typically results in more accurate analyses.

Figure 12 presents RMSEs of MVD and heights at three levels of the troposphere for case 1. The RMSEs are presented in a difference format. Specifically, each value corresponds to the RMSE between the control run and verification minus the RMSE between a satellite data run and verification, i.e.,

$$RMSE_{DF} = RMSE_{CNTL} - RMSE_{GOES} \tag{5}$$

Here,

$$RMSE_x = \sqrt{\left[\frac{1}{N}\sum^{N}\left(x - x_{verif}\right)\right]^2 + SD^2} \tag{6}$$

where N is the number of observations, SD is the standard deviation, X is a model variable from CNTL or one of the GOES wind simulations (SNGL, MULT, SLCT), and X_{verif} is a model variable from the verification analysis. Thus, negative (positive) values indicate that CNTL was closer to (further from) the verification than the simulations that included GOES winds. Since the verification data is based on a numerical model (i.e., the ECMWF), it is associated with some analysis error. Therefore, it is difficult to determine the exact error associated with the various simulations. However, if the verification analysis errors are assumed to be relatively small and consistent with time, the general characteristics of the results can still be determined.

The RMSEs of the MVD indicate similar trends between the three simulations (Figs. 12a-c). For example, at lower and upper levels (Fig. 12a,c), the simulations with GOES winds are initially inferior to CNTL (this may be a result of the aforementioned verification analysis error and/or an adjustment of the model to the 12-h forcing of GOES winds), but consistently improve with time during the forecast. At mid levels, the simulations indicate a degradation compared to CNTL during the initial 12-h, but thereafter, a gradual improvement with time is present (Fig. 12b).

Over the initial 36-h, mid- and upper-level height fields (Fig. 12d,e) contain similar characteristics to those of the mid-level MVD (Fig. 12b). Specifically, the simulations that used GOES winds degrade the forecast relative to CNTL during the initial 12 h, but then improve upon CNTL during the following 24 h. The lower-level heights are generally consistently better than CNTL during the early portion of the forecast (Fig. 12f). However, an important difference between the height and MVD fields is that the height fields indicate a marked degradation of the GOES wind cases (compared to CNTL) during the latter portion of the forecast (Fig. 12d-f). Both MULT and SLCT are generally superior to SNGL, which supports the prior evidence that GOES winds should be assimilated over multiple levels. Finally, with a few exceptions, SLCT is slightly superior to MULT, especially at mid- and upper-levels.

Case 2 is characterized by different meteorological conditions than case 1 in that rather than a strong storm progressing through the domain (Fig. 7), the conditions included only a weak and

slowly moving frontal system (Fig. 9). Therefore, it is not possible to display a track plot similar to that of case 1(Fig. 10). However, mean statistics were calculated as they were in case 1 and are presented in Fig. 13. Results at upper-levels (Fig. 13a,d) indicate that the simulations using GOES winds are initially better than CNTL, but improvement lessens between 0 and ~ 24 h. However, after this period a steady improvement is present. At mid- and lower-levels, both the MVD and heights are generally better than CNTL and contain a steady improvement with time, especially after 24 h. This improvement in the height field is different than that present in case 1 where the GOES wind simulations were relatively poor near the end of the forecast (Fig. 13d-f). In addition to the better trend of the height field in case 2, the largest improvement over CNTL is also better (~ 11 m at all levels at 48 h in case 2 while only 4 m at only upper-levels at 36 h in case 1). Overall results from case 2 indicate that the use of GOES winds adds a positive impact to the simulations, and that by 48 h a relatively large improvement is present for both variables at all levels.

5. Summary and Conclusions

The error characteristics of GOES winds were investigated by statistically comparing them with collocated radiosondes. An interesting aspect of this work is that the satellite winds at each particular height assignment were compared to *all* levels of the radiosonde data in order to characterize the depth of troposphere over which GOES winds may be representative. The basis for this investigation is that GOES winds are derived from remotely sensed features that arise from radiative processes within layers of the atmosphere rather than features at a well-defined level.

The statistical comparisons confirm that GOES winds represent layers of the troposphere to varying degrees rather than specific levels. Clear-air water vapor winds represent deeper layers than do cloudy water vapor winds or infrared cloud-tracked winds. The clear-air water vapor winds can be separated into two categories that depend on the depth of troposphere represented by the wind [i.e., broad (or deep layers) and sharp (or thin layers)]. Broad profiles tend to occur when the

vertical moisture profile is smooth and uniform, containing no relative peaks. Therefore, the vertical moisture distribution can be used to determine if a relatively thin or thick layer better represents a clear-air water vapor wind.

The impact of the findings on numerical model simulations of two winter storms in the eastern Pacific Ocean were tested using the PSU/NCAR MM5 model. Case 1 includes a strong extratropical cyclone while case 2 includes a relatively weak frontal system. For both cases, four experiments were performed: 1) A control simulation that assimilated no satellite data; 2) a simulation that used the satellite data on only a single level; 3) a simulation that used all of the satellite data on multiple levels; and 4) a simulation that used all of the satellite data over multiple levels with the exception of the clear-air water vapor winds, which were distributed based on the vertical moisture profile in the model. For the strong storm in case 1, results indicated that when compared to the control simulation, the simulations that used GOES winds improved the track of the cyclone during the initial ~ 36 h of the forecast, while degrading the track between ~ 36 and ~ 48 h. The initial improvement was most likely a result of the GOES winds modifying the initial midlevel flow in the path of the cyclone. Assimilating the data on multiple levels resulted in a better storm track than using the data on only a single level. Selectively distributing the clear-air water vapor winds resulted in slight improvements over simulations in which the winds were distributed over a fixed depth.

Statistics for mean heights and wind vector differences at several selected levels also were generated for both cases. As with the storm track of case 1, it was found that using the satellite winds over multiple levels was superior to using the data on only a single level, and selectively distributing the clear-air water vapor winds based on vertical moisture profiles generally produced the best results.

This study sheds light on the characteristics of GOES winds (especially clear-air water vapor winds) and is a necessary first step in determining how to best interpret these data and use them in numerical weather prediction. A relatively simple assimilation strategy was adopted in this study

that lays groundwork for future investigations of these important data, such as three- and four-dimensional variational assimilation techniques.

Acknowledgments

We would like to thank Dr. David Stauffer of the Penn State University for his suggestions on the use of observation nudging for data assimilation. This research was conducted under the Atmospheric Dynamics Program at NASA and acknowledgement is also made to Dr. Ramesh Kakar of NASA/Headquarters for his support of this work.

REFERENCES

Anagnostou, E. N., A. J. Negri, and R. F. Adler, 1999: A satellite infrared technique for diurnal rainfall variability studies, *J. Geophys. Res.*, **104**, 31,477-31,488.

Dudhia, J., 1989: Numerical study of convection observed during the winter monsoon experiments using a mesoscale two-dimensional model. *J. Atmos. Sci.*, **46**, 3077-3107.

Dudhia, J, 1993: A nonhydrostatic version of the Penn State-NCAR mesoscale model: Validation tests and simulation of an Atlantic cyclone and cold front. *Mon. Wea. Rev.*, **121**, 1493-1513.

Farfán, L. M., and J. A. Zehnder, 1996: Orographic influence on the synoptic-scale circulations associated with the genesis of hurricane Guillermo (1991). *Mon. Wea. Rev.*, **125**, 2683-2698.

Goerss, J.S., C. S. Velden, and J.D. Hawkins, 1998: The impact of multispectral GOES-8 wind information on Atlantic tropical cyclone forecasts in 1995: Part II: NOGAPS forecasts, *Mon. Wea. Rev.*, **126**, 1219-1227.

Grell, G. A., J. Dudhia, and D. R. Stauffer, 1995: A description of the fifth-generation Penn State/NCAR Mesoscale Model (MM5). NCAR Technical Note (NCAR/TN-398+STR), 138 pp. [Available from NCAR Publications Office, P. O. Box 3000, Boulder, CO 80307-3000.]

Hayden, C. M., and T. R. Stewart, 1987: An update on cloud and water vapor tracers for providing wind estimates. *Preprints from 6th Symposium Met. Obs. And Instr.*, New Orleans, 70-75.

Hong, S. –Y., and H. –L. Pan, 1996: Nonlocal boundary layer vertical diffusion in a medium-range forecast model. *Mon. Wea. Rev.*, **124**, 2322-2339.

Kain, J. S., and J. M. Fritsch, 1992: Convective parameterization for mesoscale models: The Kain-Fritsch scheme. *The Representation of Cumulus Convection in Numerical Models*, Meteor. Monogr., No. 46, Amer. Meteor. Soc., 165-170.

Langland, R.H., Z. Toth, R. Gelaro, I. Szunyogh, M. A. Shapiro, S. J. Majumdar, R.E. Morss, G.D. Rohaly, C. Velden, N. Bond, and C.H. Bishop., 1999: The North Pacific Experiment (NORPEX-98): targeted observations for improved North American weather forecasts, *Bull. Amer. Meteor. Soc.*, **80**, 1363-1384.

Ma, X. L., T. J. Schmit, and W. L. Smith, 1999: A nonlinear physical retrieval algorithm-its application to the GOES-8/9 sounder. *J. Appl. Meteor.*, **38**, 501-513.

Menzel, W. P., and J. F. W. Purdom, 1994: Introducing GOES-I: The first of a new generation of geostationary operational environmental satellites. *Bull. Amer. Meteor. Soc.*, **75**, 757-780.

Nieman, S. J., J. Schmetz, and W. P. Menzel, 1993: A comparison of several techniques to assign heights to cloud tracers. *J. Appl. Meteor.*, **32**, 1559-1568.

Nieman, S. J., W. P. Menzel, C. M. Hayden, D. Gray, S. Warzong, C. S. Velden, and J. Daniels, 1997: Fully automated cloud-drift winds in NESDIS operations. *Bull. Amer. Meteor. Soc.*, **78**, 1121-1133.

Rao, P. A., and H. E. Fuelberg, 1997: Diagnosing convective instability from GOES-8 radiances. *J. Appl. Meteor.*, **36**, 350-364.

Schmetz, J., K. Holmlund, J. Hoffman, B. Strauss, B. Mason, V. Gaertner, A. Koch, and L. V. De Berg, 1993: Operational cloud-motion winds from meteosat infrared images. *J. Appl. Meteor.*, **32**, 1206-1225.

Soden, B. J., C.S. Velden, and R. E. Tuleya, 2000: The impact of satellite winds on experimental GFDL hurricane model forecasts, Submitted to *Mon. Wea. Rev.*

Stauffer, D. R., and N. L. Seaman, 1990: Use of four-dimensional data assimilation in a limited-area mesoscale model. Part I: experiments with synoptic-scale data. *Mon. Wea. Rev.*, **118**, 1250-1277.

Stauffer, D. R., and N. L. Seaman, 1994: Multiscale four-dimensional data assimilation. *J. Appl. Meteor.*, **33**, 416-434.

Stensrud, D. J., R. L. Gall, S. L. Mullen, and K. W. Howard, 1995: Model climatology of the Mexican monsoon. *J. Climate*, **8**, 1775-1794.

Tomassini, M. , G. Kelly, and R. Saunders, 1998: Use and impact of satellite atmospheric motion winds on ECMWF analyses and forecasts. *Mon. Wea. Rev.*, **127**, 971-986.

Troen, I., and L. Mahrt, 1986, A simple model of the atmospheric boundary layer: Sensitivity to surface evaporation. *Bound.-Layer Meteor.*, **37**, 129-148.

Turk, J., J. Vivekanandan, T. Lee, P. Durkee, and K. Nielsen, 1998: Derivation and applications of near-infrared cloud reflectances from GOES-8 and GOES-9. *J. Appl. Meteor.*, **37**, 819-831.

Velden, C.S., 1996: Winds derived from geostationary satellite moisture channel observations: applications and impact on numerical weather prediction. *Meteorol. Atmos. Phys.*, **60**, 37-46.

Velden, C.S., C.M. Hayden, S.J. Nieman, W.P. Menzel, S. Wazong, and J.S. Goerss, 1997: Upper tropospheric winds derived from geostationary satellite water vapor observations, *Bull. Amer. Meteorol. Soc.*, **78**, 173-195.

Velden, C. S., T. L. Olander, and R. M. Zehr, 1998a: Development of an objective scheme to estimate tropical cyclone intensity from digital geostationary satellite infrared imagery. *Wea. Forecasting.*, **13**, 172-186.

Velden, C.S., T.L. Olander, and S. Wazong, 1998b: The impact of multispectral GOES-8 wind information on Atlantic tropical cyclone track forecasts in 1995: Part I Dataset methodology, description and case analysis, *Mon. Weath, Rev.*,**126**, 1202-1218.

Weldon, R. B., and S. J. Holmes, 1991: Water vapor imagery: Interpretation and applications to weather analysis and forecasting. NOAA Tech. Rep. NESDIS 67, 213 pp. [Available from NOAA Science Center, 5200 Auth Rd., Camp Springs, MD 20748.]

FIGURE CAPTIONS

1. a) RMSE (m s^{-1}) between GOES winds and collocated RAOBs at individual height assignment level. b) As in panel a, but normalized RMSE.
2. RMSE (m s^{-1}) between 300 hPa GOES winds and *entire* profile of collocated RAOBs.
3. a) RMSE (m s^{-1}),mean dewpoint depression (DD) (K), and mean dewpoint depression gradient (DDG) (5 X K hPa^{-1}) within "broad" category of CA WV winds at a height assignment of 300 hPa. b) As in panel a but for "sharp" category. Bottom three panels contain representative profiles of the vector difference (panel c, m s^{-1}), DD (panel d, K), and DDG (panel e, K hPa^{-1}). Vertical dash-dot line in panels a, b, and e indicates a value of zero.
4. As in Fig. 3 but for 400 hPa height assignments. Also included in panels c-e is a typical "multi-peaked" profile.
5. a) "Broad" CA WV profile (Fig. 3a) for 300 hPa height assignments along with corresponding "NC" profiles (m s^{-1}) as described in the text. b) As in panel a but for "sharp" category.
6. Domain for model simulations.
7. ECMWF model analyses of mean sea level pressure (hPa) at 1200 UTC 28 January (panel a), 0000 UTC 29 January (panel b), and 1200 UTC 31 January 2000 (panel c). Points A, B, and C represent series of cyclones that were present during the simulation.
8. GOES-10 water vapor image at 0000 UTC 29 January 2000.

9. ECMWF model analyses of mean sea level pressure (hPa) at 1200 UTC 16 January (panel a), 0000 UTC 18 January (panel b), and 0000 UTC 19 January 2000 (panel c). Dotted lines indicate frontal positions.

10. Tracks of cyclone within four simulations at 12-hour intervals. Also included is the observed track.

11. Minimum mean sea level pressure (hPa) of storm during forecast within each simulation.

12. Improvement over control run of SNGL (thin solid line), MULT (dashed line) and SLCT (thick solid line), of mean vector difference (m s^{-1}) and heights (m) at 300 (panels a,d), 500 (panels b,e) and 850 hPa (panels c,f). Values consist of RMSE between verification data and CNTL minus RMSE between verification data and SNGL,MULT, or SLCT. Positive values indicate an improvement (compared to CNTL), while negative values indicate a degradation (compared to CNTL). Horizontal dash-dot line indicates value of zero.

13. As in Fig. 13 but for case 2.

Table 1. Experiments described in text.

Experiment	Assimilation	Winds Assimilated	Depth of Layer
CNTL	NO	-----	-----
SNGL	YES	ALL	-----
MULT	YES	ALL	150 hPa
SLCT	YES	ALL	150 hPa or 250 hPa*

*If model moisture profile is similar to that of "broad" category, clear-air water vapor wind is distributed over 250 hPa layer.

Fig. 1

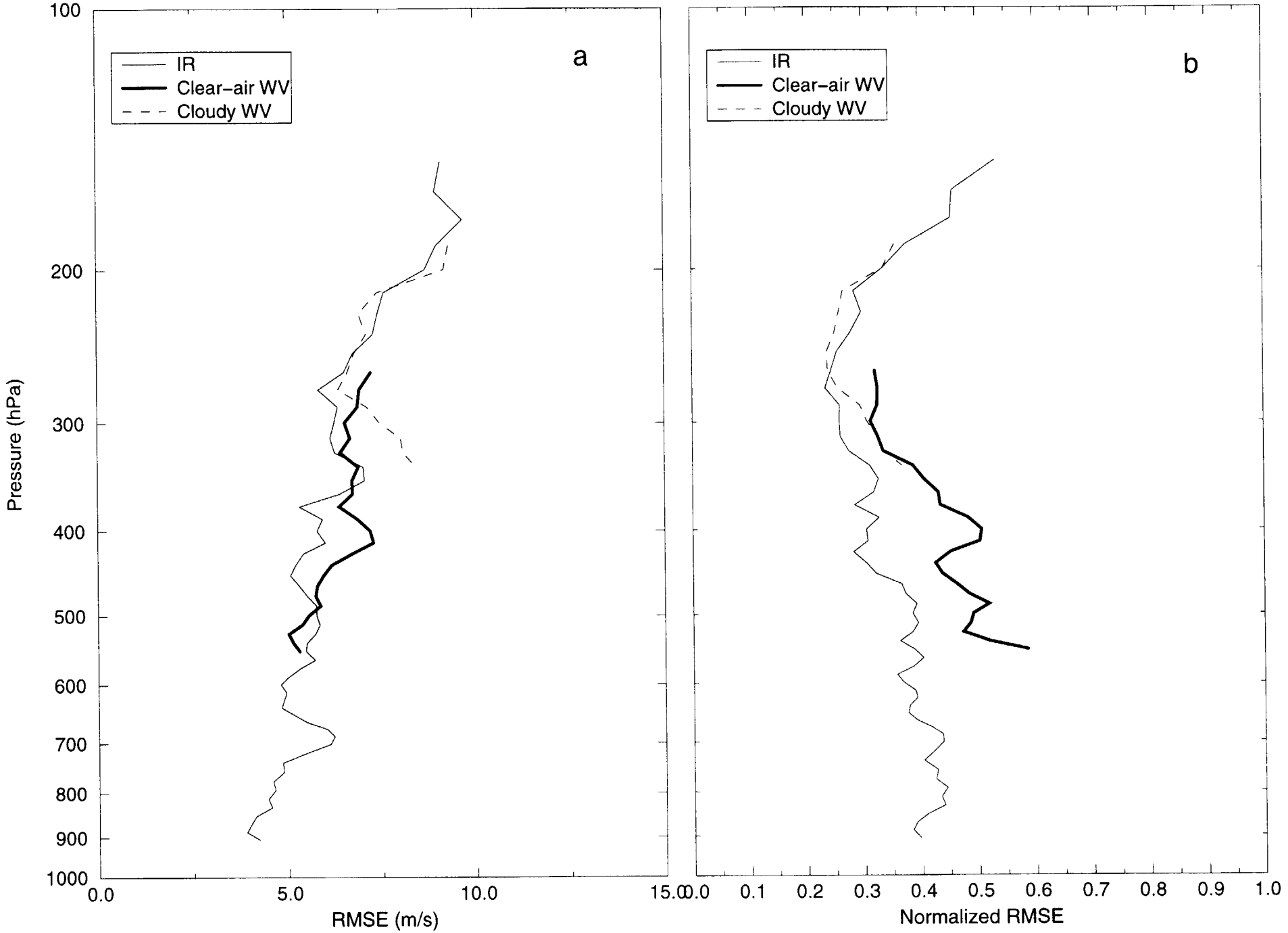
a
b
IR
Clear-air WV
Cloudy WV
Pressure (hPa)
100
200
300
400
500
600
700
800
900
1000
0.0
5.0
10.0
15.0
RMSE (m/s)
0.0
0.1
0.2
0.3
0.4
0.5
0.6
0.7
0.8
0.9
1.0
Normalized RMSE

Fig. 2

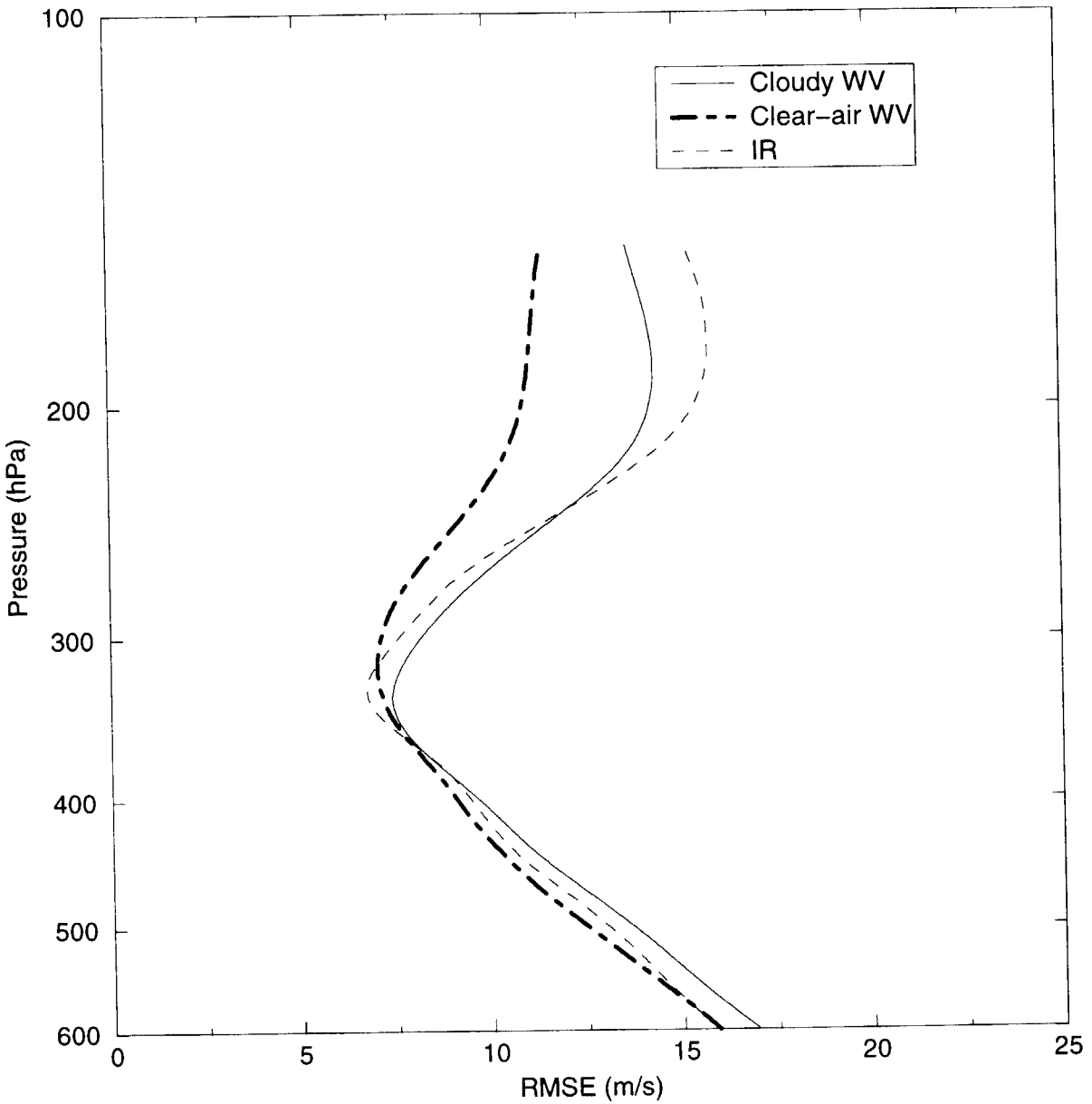
Cloudy WV
Clear–air WV
IR
Pressure (hPa)
100
200
300
400
500
600
0
5
10
15
20
25
RMSE (m/s)

Fig. 3

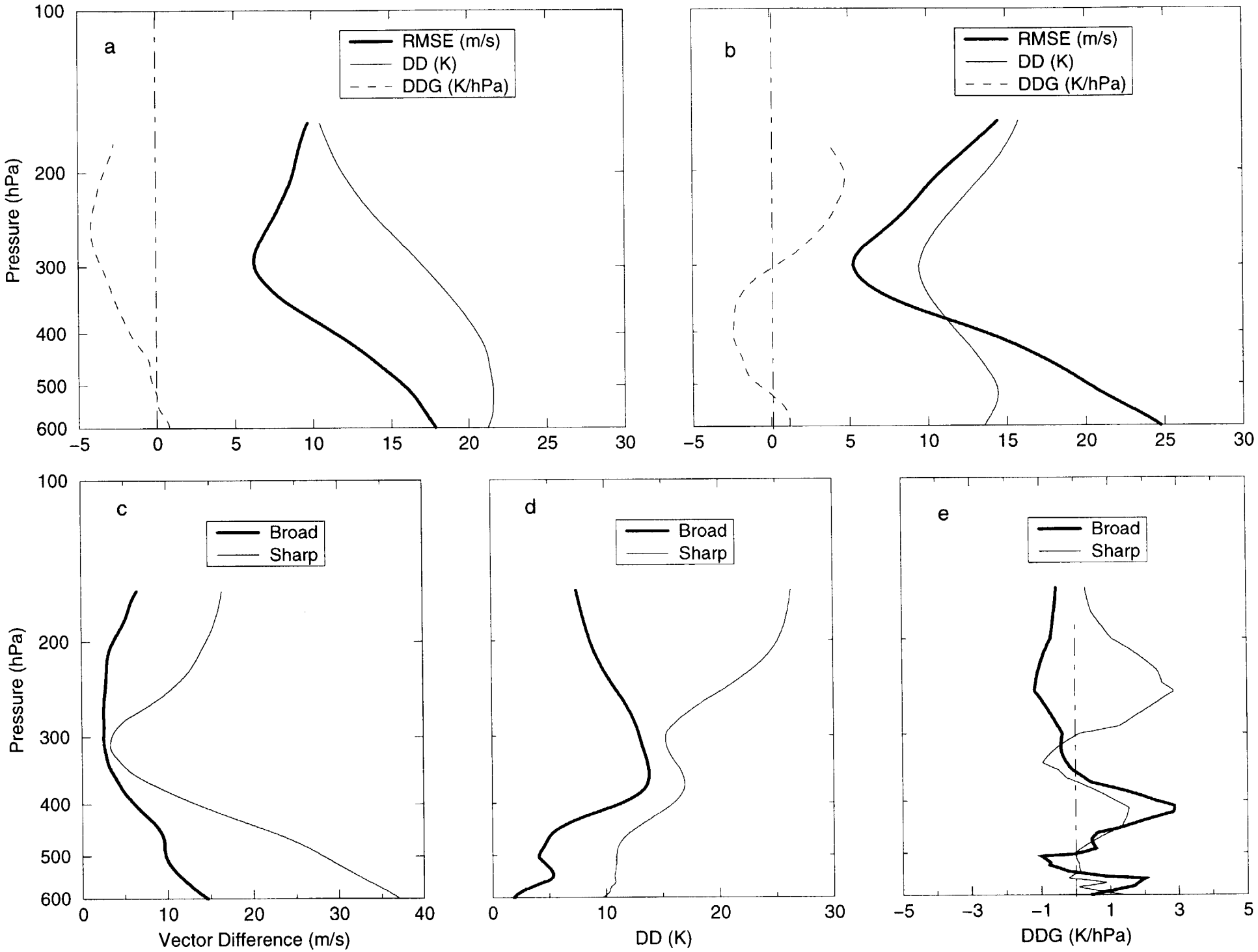
a
RMSE (m/s)
DD (K)
DDG (K/hPa)
b
RMSE (m/s)
DD (K)
DDG (K/hPa)
Pressure (hPa)
100
200
300
400
500
600
−5
0
5
10
15
20
25
30
c
Broad
Sharp
d
Broad
Sharp
e
Broad
Sharp
0
10
20
30
40
Vector Difference (m/s)
0
10
20
30
DD (K)
−5
−3
−1
1
3
5
DDG (K/hPa)

Fig. 4

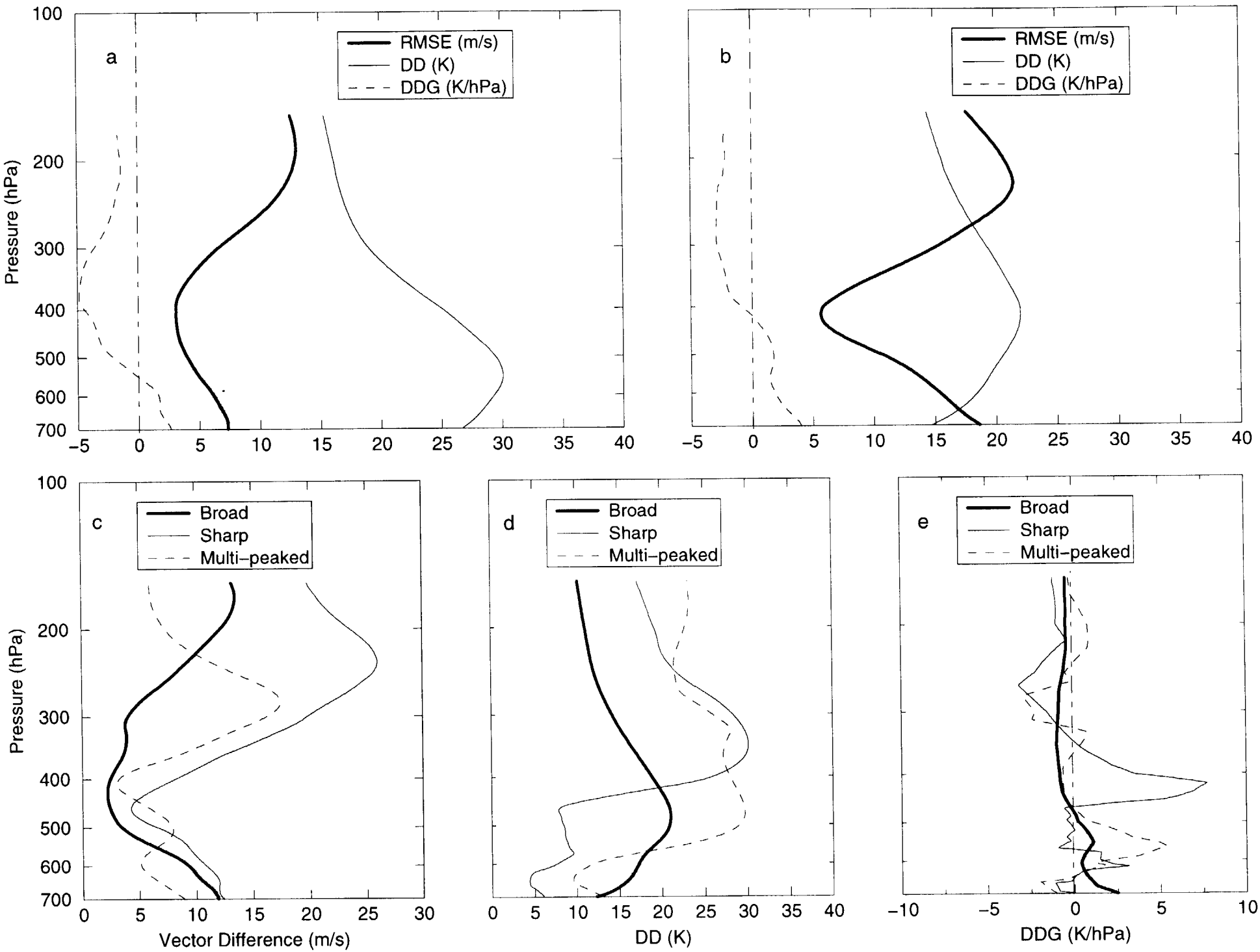
a
RMSE (m/s)
DD (K)
DDG (K/hPa)
Pressure (hPa)
100
200
300
400
500
600
700
−5
0
5
10
15
20
25
30
35
40
b
RMSE (m/s)
DD (K)
DDG (K/hPa)
c
Broad
Sharp
Multi−peaked
Pressure (hPa)
0
5
10
15
20
25
30
Vector Difference (m/s)
d
Broad
Sharp
Multi−peaked
0
5
10
15
20
25
30
35
40
DD (K)
e
Broad
Sharp
Multi−peaked
−10
−5
0
5
10
DDG (K/hPa)

Fig. 5

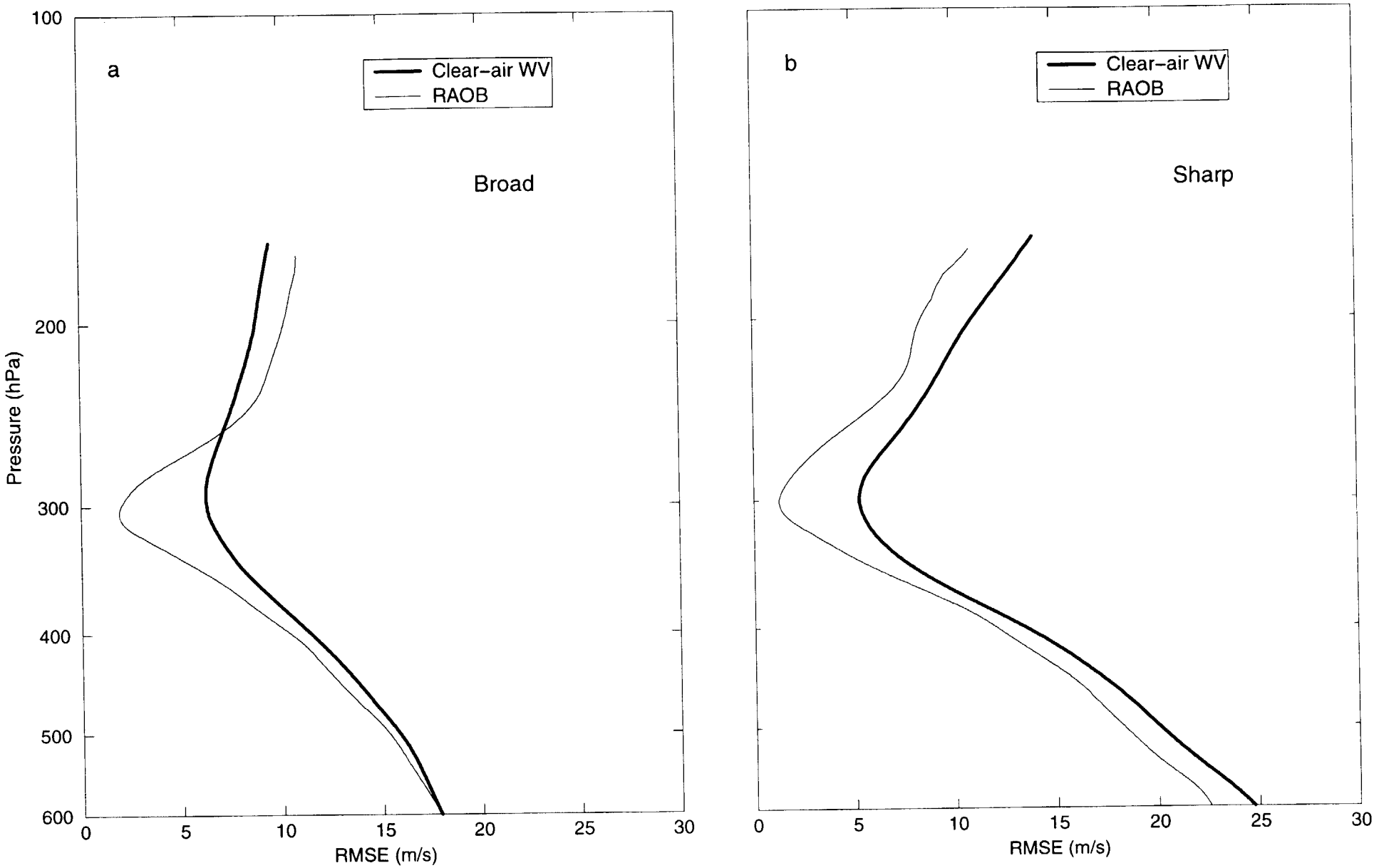
a
Clear–air WV
RAOB
Broad
Pressure (hPa)
100
200
300
400
500
600
0
5
10
15
20
25
30
RMSE (m/s)
b
Clear–air WV
RAOB
Sharp
0
5
10
15
20
25
30
RMSE (m/s)

Fig. 6

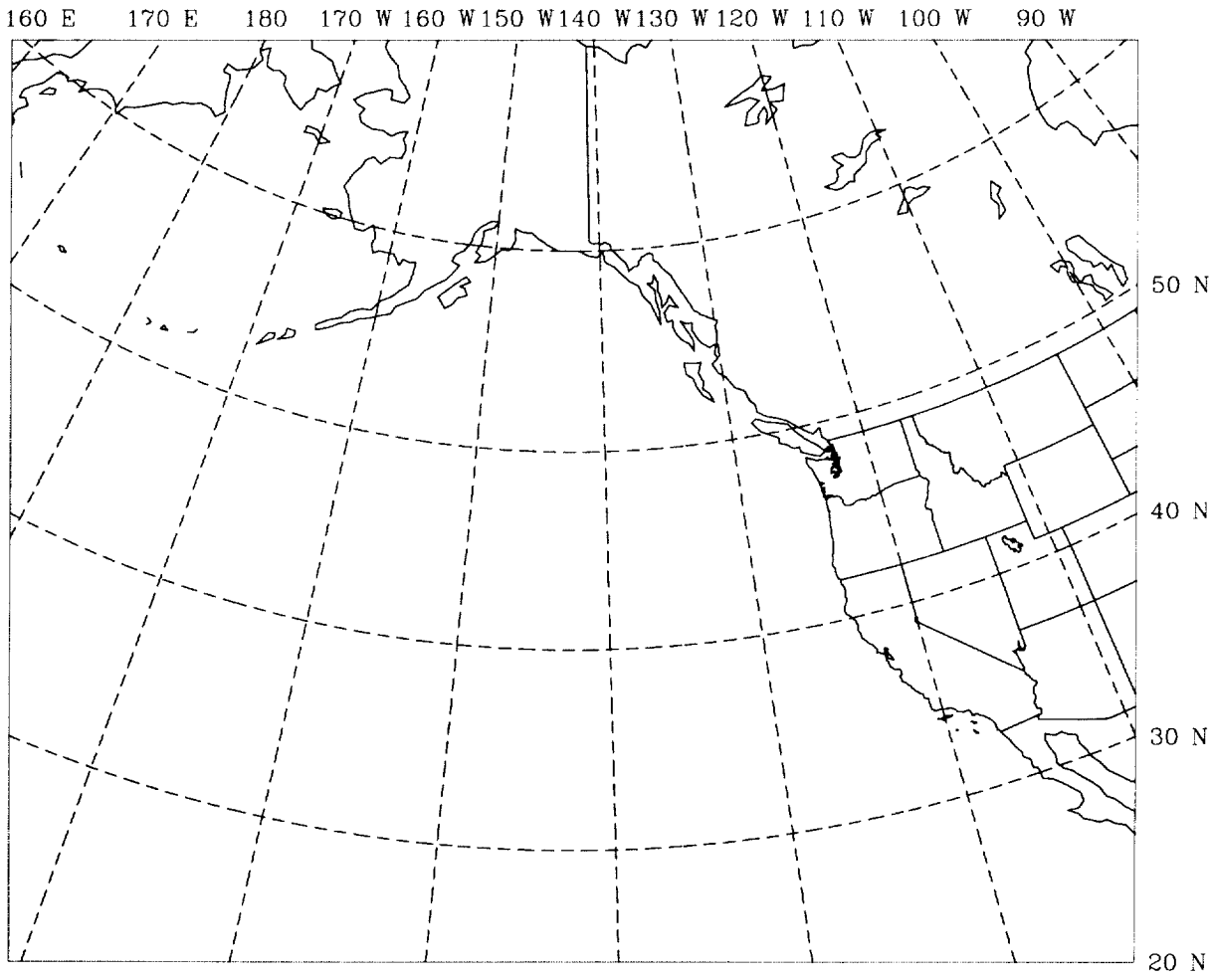
160 E
170 E
180
170 W
160 W
150 W
140 W
130 W
120 W
110 W
100 W
90 W
50 N
40 N
30 N
20 N

Fig. 7

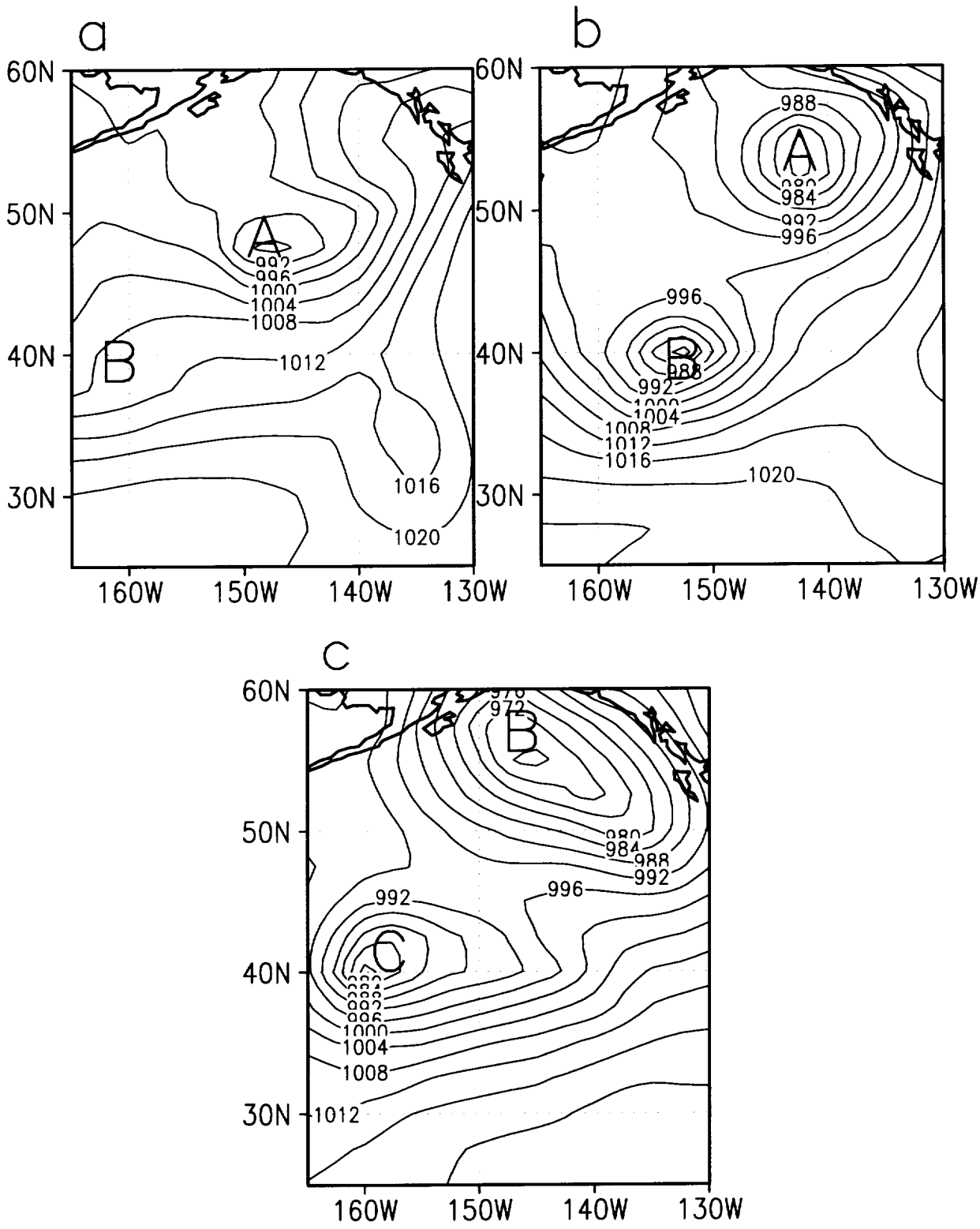
a
60N
50N
40N
30N
160W
150W
140W
130W
A
B
992
996
1000
1004
1008
1012
1016
1020
b
988
984
992
996
1000
1004
1008
1012
1016
1020
c
976
972
980
984
988
992
996
1000
1004
1008
1012

Fig. 8

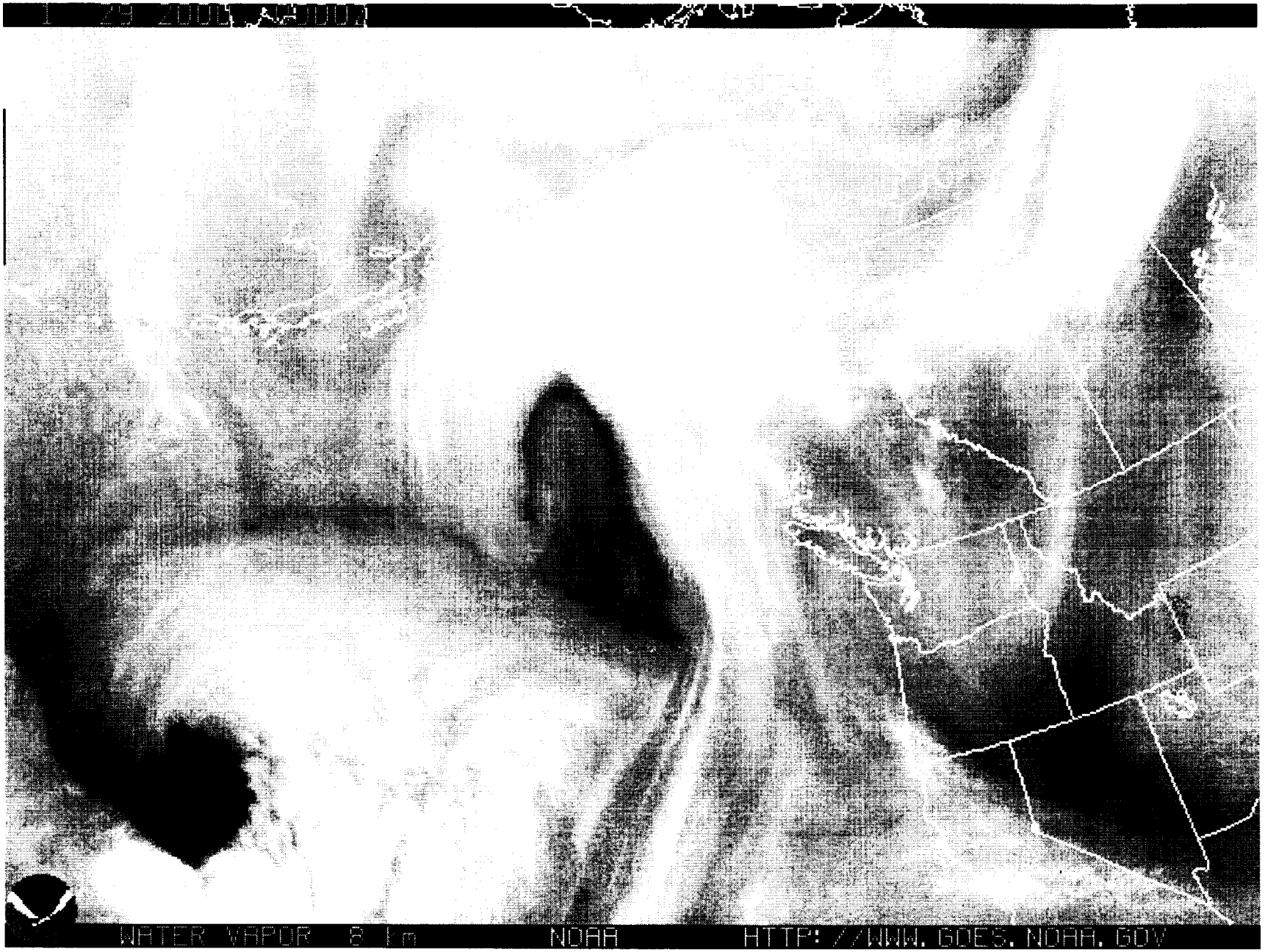

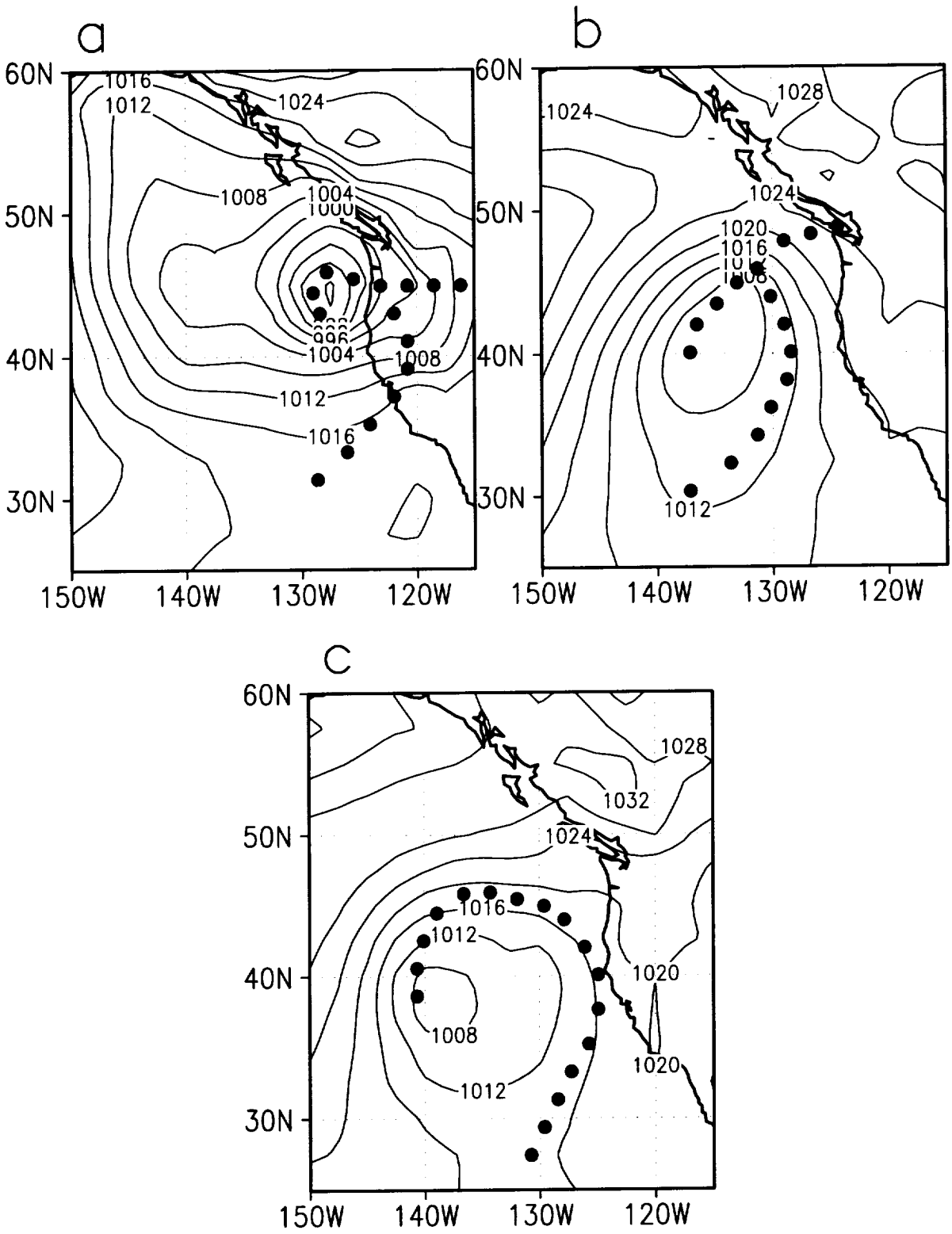
a
60N
50N
40N
30N
150W
140W
130W
120W
1016
1012
1024
1008
1004
1000
996
1004
1008
1012
1016
b
60N
50N
40N
30N
150W
140W
130W
120W
1028
1024
1024
1020
1016
1012
c
60N
50N
40N
30N
150W
140W
130W
120W
1028
1032
1024
1016
1012
1020
1008
1020
1012

Fig. 10

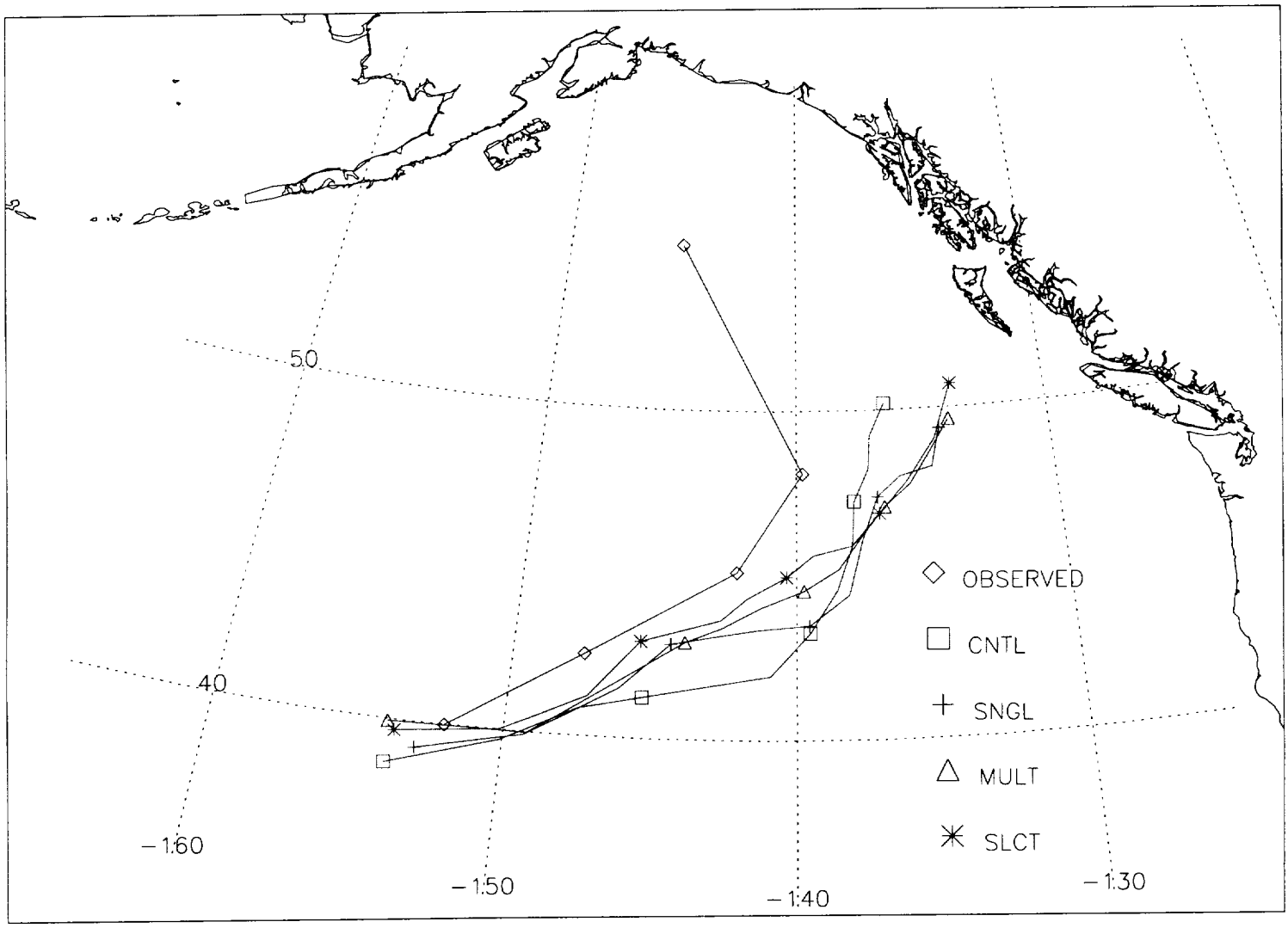

Fig. 11

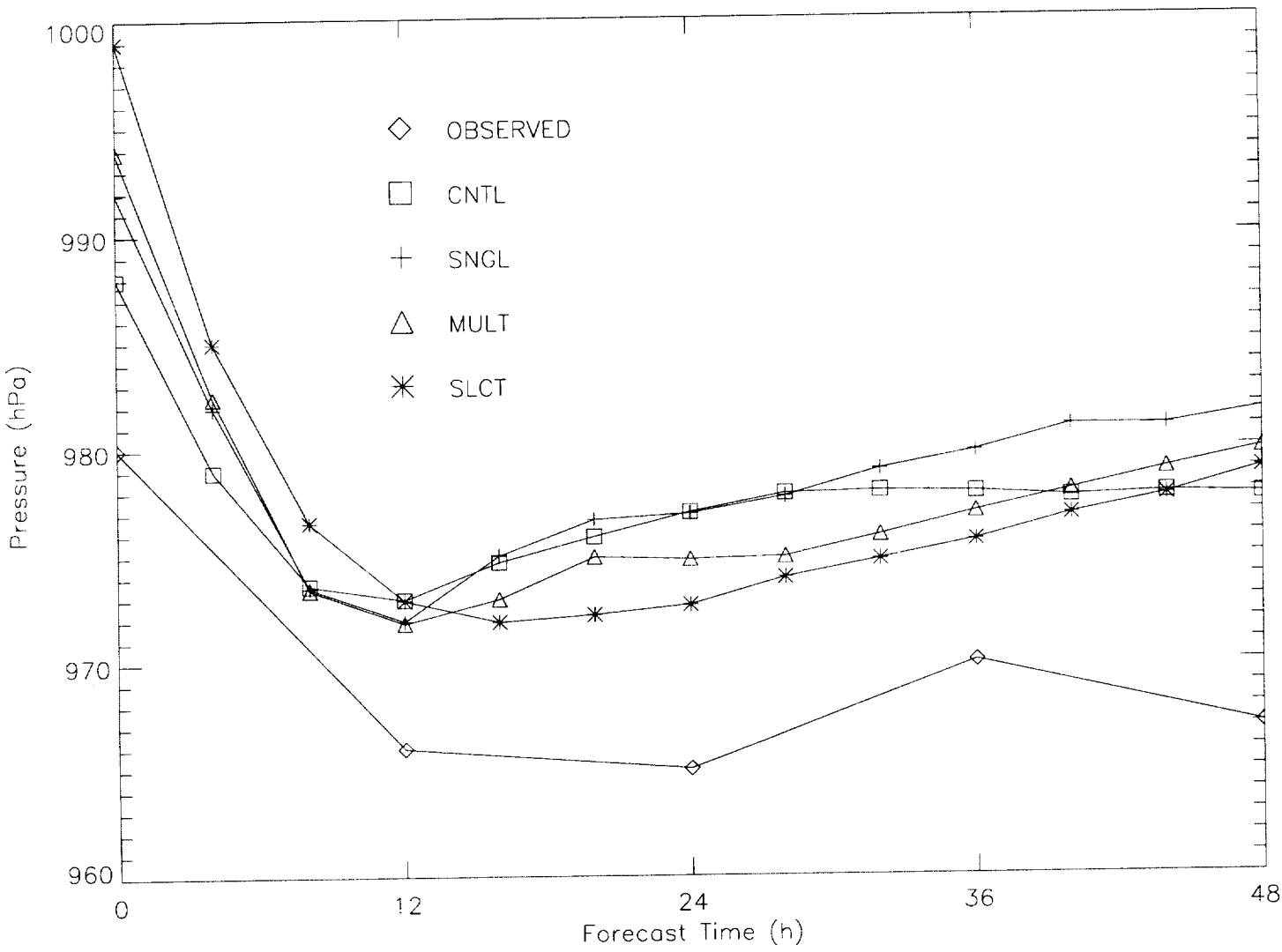
1000
990
980
970
960
Pressure (hPa)
0
12
24
36
48
Forecast Time (h)
OBSERVED
CNTL
SNGL
MULT
SLCT

Fig. 12

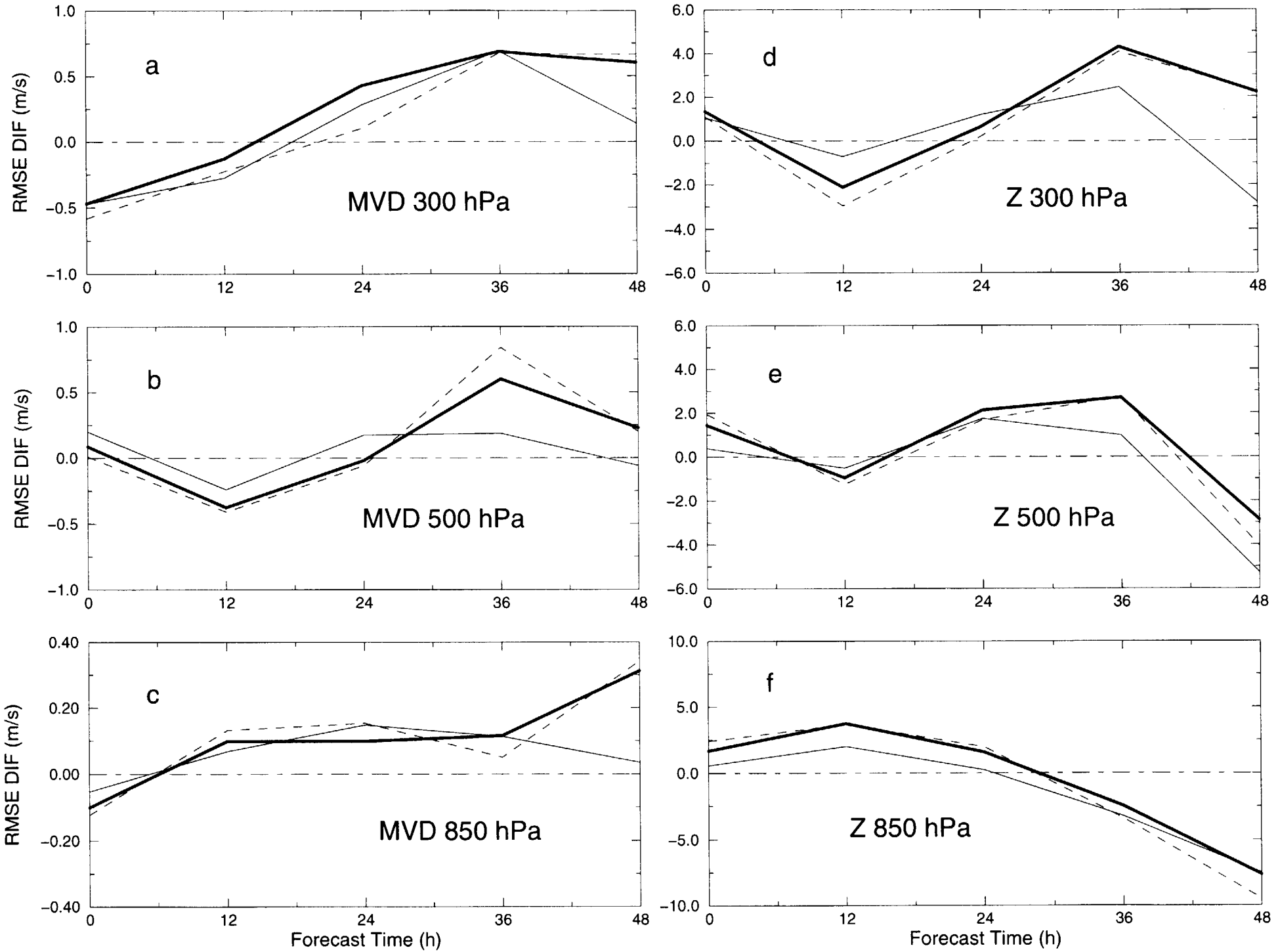
a
MVD 300 hPa
b
MVD 500 hPa
c
MVD 850 hPa
d
Z 300 hPa
e
Z 500 hPa
f
Z 850 hPa
RMSE DIF (m/s)
RMSE DIF (m/s)
RMSE DIF (m/s)
Forecast Time (h)
Forecast Time (h)
1.0
0.5
0.0
-0.5
-1.0
6.0
4.0
2.0
0.0
-2.0
-4.0
-6.0
0.40
0.20
0.00
-0.20
-0.40
10.0
5.0
0.0
-5.0
-10.0
0
12
24
36
48

Fig. 13

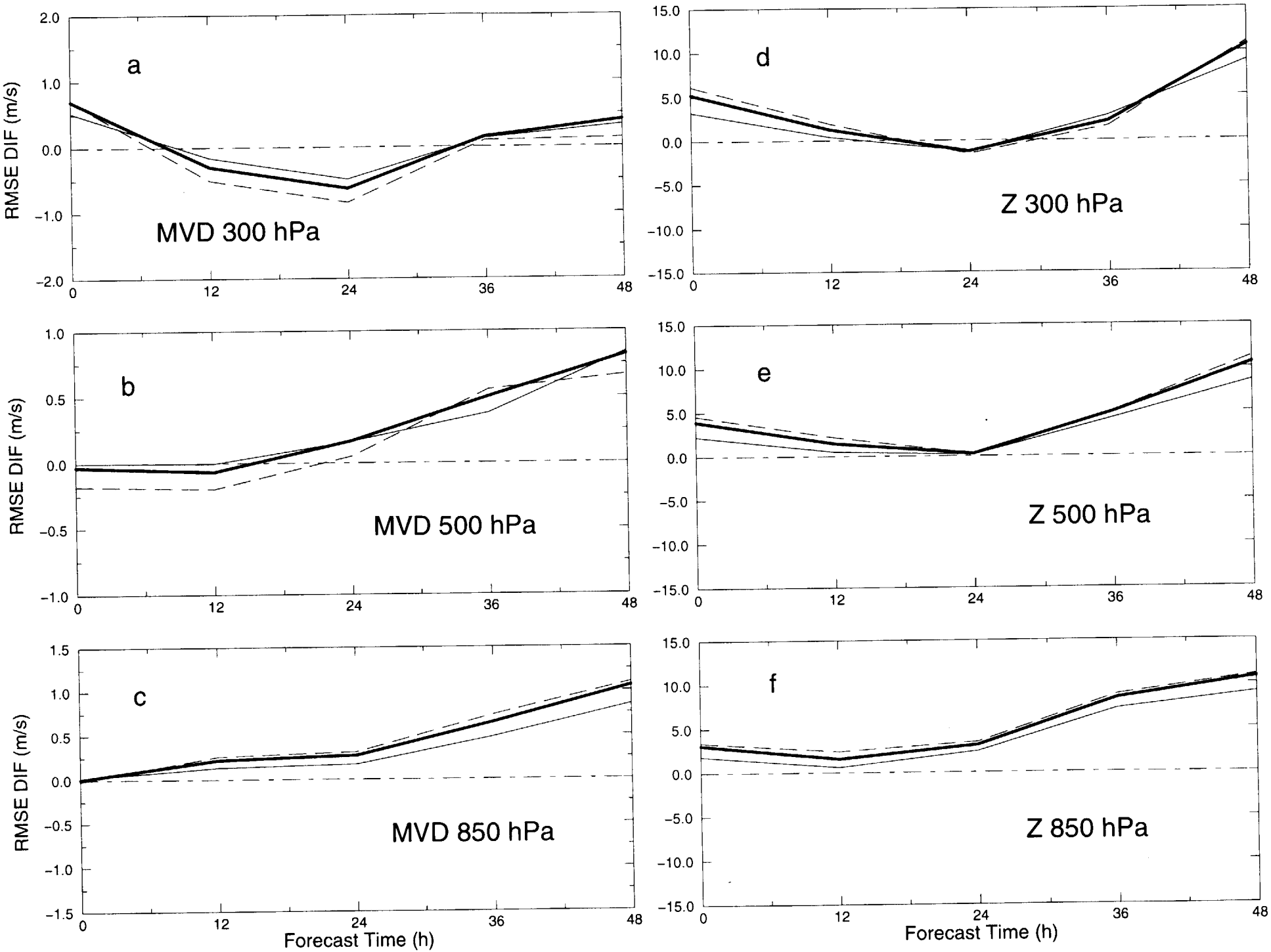
a
MVD 300 hPa
d
Z 300 hPa
b
MVD 500 hPa
e
Z 500 hPa
c
MVD 850 hPa
f
Z 850 hPa
RMSE DIF (m/s)
Forecast Time (h)